SMART SYSTEM FOR VEHICLE COMFORT MONITORING AND ACTIVE SUSPENSIONS CONTROL

Aleksandar Peulić [1], *Željko Jovanović* [2]

UDC:629.113;534.015.1

1. INTRODUCTION

Vehicle movement over random road surface produces oscillations that impact on passengers and a vehicle. Generally, it is accepted that the vibrations which passengers feel during the ride has the greatest impact on passenger comfort. This field is known as whole-body vibration (WBV). Current standards and regulations for WBV are defined in:

- ISO standard 2631–1 (1997), [1]
- British Standard 6841 (1987), [2]
- ANSI S3.18:2002 [3]
- European Directive 2002/44/EC [4]
- The Control of Vibration at Work Regulations [5].

An overview of current standard and regulations is presented in [6]. The International Standard Organization (ISO) presents a criterion for ride comfort evaluation (ISO 2631) [1] which describes the effects of vibrations on a person.

Both standards and regulations assume that acceleration magnitude, frequency spectrum, and duration represent the principal exposure variables, which account for the potential harmful effects. At the national level in Serbia there is standard ICS 13.160 (SRPS ISO 2631-1:2014 Mechanical vibration and shock: Evaluation of human exposure to whole-body vibration, Part 1: General requirements). Besides vibration exposure, duration and direction of a vibration exposure are important for passengers comfort. According to the ISO 2631-1 standard [1], whole-body vibration exposure is a health risk. Many jobs are exposed to vibrations. Authors of [7] use ISO 2631 standard method for whole-body vibration exposure in comfort determination for haulage truck operators in surface mining operations. They showed that workers were exposed to WBV levels that exceeded safety limits, as dictated by the ISO 2631-1 standard. The authors of [8] showed little match between ISO 2631-1 comfort prediction results and self-reported results during heavy machinery routines for construction, forestry, and mining vehicles. In [9] authors presented a high correlation between whole-body vibration exposure and disability pension retirement, while the authors of [10] concluded that mechanical vibrations affects more on older and lighter drivers .

There are two ways to reduce the oscillations. First one is to build good quality roads, and the second one is development of the suspension systems. Classic suspension systems, produced only with the springs and shock absorbers, cannot change their

[1] *Aleksandar Peulić, Assist. prof., University of Kragujevac, Faculty of Engineering, Serbia, Sestre Janjić 6, 34000 Kragujevac, aleksandar.peulic@kg.ac.rs*
[2] *Željko Jovanović, Teaching assist., University of Kragujevac, Faculty of Technical Sciences, Čačak, Serbia, Svetog Save 65, 32000 Čačak, zeljko.jovanovic@ftn.kg.ac.rs*

characteristics during the transport. They are created to produce compromise between comfort and vehicle stability.

Linear optimal control [11] is part of the modern control theory which enables the design of specific types of analytical systems. This is applied in [12, 13] for the optimal design of active vehicle suspension system based on the use of the feedback loop. In [12] active suspension system is realized by using multivariate interactive PI control. Problem with this method it that it is necessary to measure suspension stroke, tire stroke and speed of a suspended and unsuspended mass. In [13] is designed regulator with full observer, which in the feedback use estimated states instead the real ones. Measurement of only one parameter, suspension stroke, is needed. By enabling integrators in the feedback loop, per output, by including the state variable which represent the integral of the output (ie. the suspension stroke) of the system, the prime response output in a stationary mode, at constant excitation force acting on the suspended mass and the input from the road surface is achieved.

Nowadays, accelerometers and GPS are part of almost every smart phone. This is the main reason for becoming interesting as mobile sensing devices. Mobile technologies may have the potential in becoming the leader of data gathering in this field. Paper [14] described a mobile sensing system for road irregularity detection using Android OS-based smartphones. Paper [15] considered the problem of monitoring road and traffic conditions in a city using smartphones.

This paper describes the design of the controller which is based on an approach [13], except estimation of the measurable state variable. For testing purposes smart system for acceleration measurement in form of Android application is developed. Nowadays, accelerometers, gyroscope and GPS are part of almost every smart phone. This is the main reason they are becoming interesting as mobile monitoring devices in transportation. The authors of [3] used high-pass filtered accelerometer data in order to detect road potholes. Paper [6] described a mobile sensing system for road irregularity detection using Android OS-based smartphones. Paper [7] also considered the problem of monitoring road and traffic conditions in a city using smartphones. For simulation, two scenarios are created: “ramp” – hitting the surface with angle slope, “step” – hitting the curb.

2. FORMULATION OF THE PROBLEM

We will assume that the active suspension system contains conventional elements (spring and shock absorber) with hydraulic or electro-hydraulic actuator. We look at a simplified, linear "quarter car" model of vehicle presented on the Figure 1. For this model and its dynamic environment, we define the differential matrix equation:

$$\dot{x} = Ax + bu + Zw \tag{1}$$

where the system matrix are:

$$A=\begin{bmatrix} 0 & 0 & 1 & -1 \\ 0 & 0 & -1 & 0 \\ -\frac{\lambda_2}{m_1} & \frac{\lambda_1}{m_1} & -\frac{\beta_2}{m_1} & \frac{\beta_2}{m_1} \\ \frac{\lambda_2}{m_2} & 0 & \frac{\beta_2}{m_2} & -\frac{\beta_2}{m_2} \end{bmatrix} \qquad b=\begin{bmatrix} 0 \\ 0 \\ -\frac{1}{m_1} \\ \frac{1}{m_2} \end{bmatrix} \tag{2}$$

$$Z=\begin{bmatrix} 0 & 0 \\ 1 & 0 \\ 0 & 0 \\ 0 & -\frac{1}{m_2} \end{bmatrix} \qquad w=\begin{bmatrix} \dot{x}_0 \\ f \end{bmatrix}$$

x is the state vector of the fourth order, u is the scalar control force, and w is a vector of input.

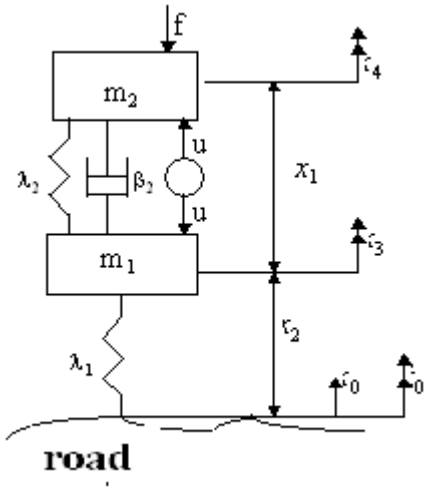

Figure 1 A quarter-car model of suspension system

The output of the system is one variable, suspension stroke:

$$y=Cx \qquad \text{where c is:} \qquad C=\begin{bmatrix} 1 & 0 & 0 & 0 \end{bmatrix} \tag{3}$$

Also, it is necessary to neutralize the constant impact of the system disorders vector w (static force f acting on the suspended weight and "ramp" from the road surface) in stationary mode.

Therefore, it is necessary to expand the state vector of the system (1) and introduce a new state variable, g(t):

$$\dot{g} = y \tag{4}$$

which represents the integral of the output (3) of the system. Extended system can be described with matrix equations:

$$\begin{aligned} \dot{\tilde{x}} &= \tilde{A}\tilde{x} + \tilde{b}u + \tilde{Z}w \\ y &= \tilde{C}\tilde{x} \end{aligned} \tag{5}$$

where the matrix and vectors are formed in the following manner:

$$\tilde{x} = \begin{bmatrix} x \\ g \end{bmatrix} \tilde{A} = \begin{bmatrix} A & 0 \\ C & 0 \end{bmatrix} \tilde{b} = \begin{bmatrix} b \\ 0 \end{bmatrix} \tilde{Z} = \begin{bmatrix} Z \\ 0 \end{bmatrix} \tilde{C} = \begin{bmatrix} C & 0 \end{bmatrix} \tag{6}$$

3. OPTIMAL LINEAR CONTROL

Selection of the Riccati state controller for solving problems of optimization of the complete system provides the analytical solution with a relatively short period of time necessary for the design and calculation. This type of controller takes, calculates and return system state, which is an advantage over some classic regulator structures.

By minimizing the linear quadratic performance index leads to the law of control in a closed loop by state. For expanded system (5) performance index penalizes non-zero status and management, ie. takes into account the limited suspension workspace, stability of the vehicle on the road and ride comfort of passengers.

In matrix form, the performance index is given by the equation:

$$J = \frac{1}{2}\int_0^\infty \left[\tilde{x}^T Q \tilde{x} + \rho u^2\right] dt \tag{7}$$

where is:

$$Q = \begin{bmatrix} q_1 & 0 & 0 & 0 & 0 \\ 0 & q_2 & 0 & 0 & 0 \\ 0 & 0 & 0 & 0 & 0 \\ 0 & 0 & 0 & 0 & 0 \\ 0 & 0 & 0 & 0 & q_3 \end{bmatrix} \tag{8}$$

Different choice of weights coefficients in the index performance (7) can provide different control, ie. different system performance. By solving Riccati algebraic matrix equation:

$$P\tilde{A} + \tilde{A}^T P - P\tilde{b}\rho^{-1}\tilde{b}^T P + Q = 0 \tag{9}$$

which solution is symmetric positive definite matrix P, we get the optimal control equations:

$$u = -\rho^{-1}\tilde{b}^T P\tilde{x} \tag{10}$$

and row-matrix of the Kalman amplification in the feedback is:

$$K = \rho^{-1}\tilde{b}^T P \tag{11}$$

and can be divided into proportional and integral amplification:

$$K = \begin{bmatrix} K_p & K_i \end{bmatrix} \tag{12}$$

so that the control rules (10) can be written in the form:

$$u = -K_p x - K_i g \tag{13}$$

It is easy to show that the system is in closed loop (when all states are measurable),

$$\dot{\tilde{x}} = \left(\tilde{A} - \tilde{b}K\right)\tilde{x} + \tilde{Z}w \tag{14}$$

asymptotically stable.

4. REDUCED OBSERVER

In the case of a system in which all states measurements are not available in a simple and easy way, very often the state observer is projected that estimate the state of the system based on the measurement and control of outputs [4]. Estimated states are used instead of the real ones for obtaining control (13), which is justified by the separation theorem [1].

In the adopted model, Figure 1, is a fourth order system with the one measurable state variable so is necessary to design a reduced third-order observer [5]. For ease of performing a mathematical relationship, we will simply break down the state vector on:

$$x' = x_1 \qquad x'' = \begin{bmatrix} x_2 & x_3 & x_4 \end{bmatrix}^T \tag{15}$$

and system matrixes (2), so we have:

$$\begin{aligned} \dot{x}' &= A_{11}x' + A_{12}x'' + b_1 u + Z_1 w \\ \dot{x}'' &= A_{21}x' + A_{22}x'' + b_2 u + Z_2 w \end{aligned} \tag{16}$$

Vector of the estimated states is defined by the equation:

$$x_e'' = h + Lx' \tag{17}$$

where *h* is new 3-dimensional state vector system, and ***L*** is the amplifying vector of the reduced observer which need to be calculated. By swapping (17) in (16) instead of the x'', and eliminating disturbance vector, we obtained:

$$\dot{h} = A_{21}x' + \left(A_{22} - LA_{12}\right)x_e'' + b_2 u \tag{18}$$

Figure 2 shows the way of designing the reduced observer. Control is given by equation:

$$u = -K_p' x' - K_p'' x_e'' - K_i g \tag{19}$$

where KP is:

$$K_p = \begin{bmatrix} K_p' & K_p'' \end{bmatrix} \tag{20}$$

Figure 3 shows the realization of complete systems with closed feedback loop.

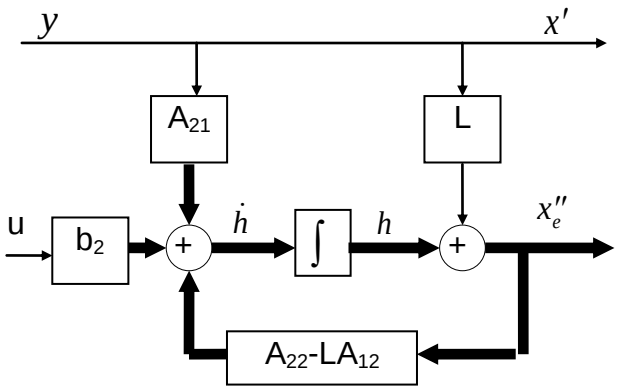

Figure 2 Generating of the immeasurable estimated states

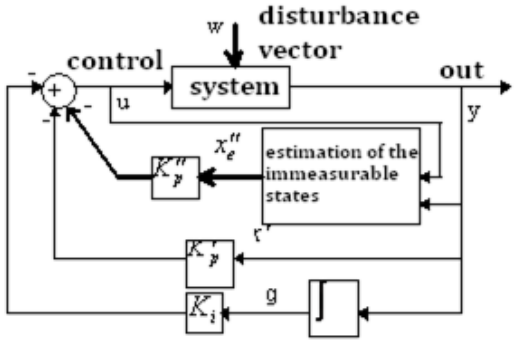

Figure 3 System with the closed feedback loop

Estimation error of the immeasurable states is denoted by the:

$$\varepsilon'' = x'' - x_e'' \tag{21}$$

then from the equations (16) and (17), by subtracting and using equation (18), we get the differential equation for the estimation errors (21):

$$\dot{\varepsilon}'' = \left(A_{22} - LA_{12}\right)\varepsilon'' + Z_2 w \tag{22}$$

According to the separation characteristic, set of values consists of the system values and the reduced observer values which are zeros s_{ir} , i=1,2,3, of polynomial:

$$\det\left(sI - A_{22} + LA_{12}\right) = 0 \tag{23}$$

arbitrarily are set by selecting the appropriate amplifying value of the reduced observer.

If we assume that the system does not operate with disorders and if self-worth values of the observer (23) have negative real parts, error estimation (21), (22) will tend to zero according to an exponential law, and x_e'' will follow the x'' after a certain time (which depends on the observer's values). At first glance, it is best to choose such observer amplification **L** that the observer's own values have high negative real parts:

$$\mathrm{Re}\left(s_{ir}\right) << \mathrm{Re}\left(s_{js}\right) < 0 \tag{24}$$

where s_{js} , j=1..4 are own system values (14), ie. zero polynomial:

$$\det\left(sI - A + bK_p\right) = 0 \tag{25}$$

because then estimated sheet (17) start to follow real states (15), as fast as possible. But, from the other side, higher observer values, in the left half plane, the bandwidth of the observer is higher, and the effect of measurement noise is higher on the result of estimation. Thus, the impact of noise on the measurement system that determines the upper limit of the speed with which the estimated states can approach to the real states. Therefore, the design of the observer consists in seeking and finding a compromise between the estimation speed and performance loss due to noise on the measurement system.

5. ANDROID APPLICATION

Android application is developed to monitor transport parameters using accelerometer and GPS (for storing location). Main application functionalities are developed using RxJava [17] for accelerometer calculations, GPS monitoring, and main application in the separate threads. The developed Android application algorithm is presented in Figure 4.

After application parameters setup, the accelerometer and GPS threads start. Next step is accelerometer calibration, and after that, the comfort calculation is performed. During calculations, the accelerometer axis live signals are plotted on the phone display. After the decision time interval has passed, the user needs to choose subjective comfort level (comfortable, little uncomfortable, and very uncomfortable). Calculated data are stored to files while new calculations starts in the background.

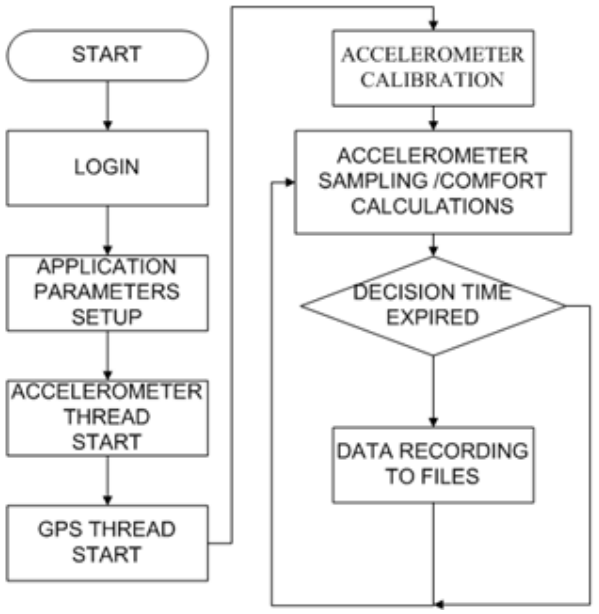

Figure 4 Algorithm of usage for the developed Android application

In order to measure the dynamic accelerations of the device, the influence of the force of gravity must be eliminated. This is achieved by applying a high-pass filter over raw accelerometer data, according to equation (26):

$$HPX_i = HPX_{i-1} - ((RX \cdot fc) + HPX_{i-1} \cdot (1 - fc)) \tag{26}$$

where HPXi is the i-th high-pass-filtered X axis acceleration, RX is raw X axis acceleration data, and fc=0.1 is the filter coefficient that cuts the 10% of the lower frequencies. Raw and filtered data for all three axes are presented in Figure 5.

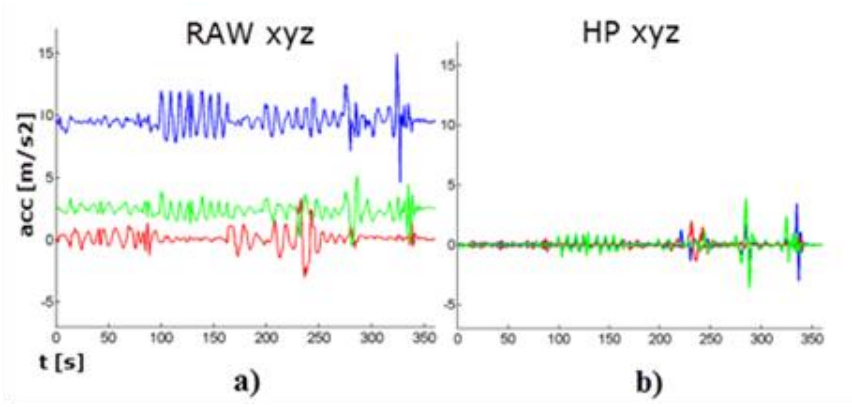

Figure 5 Raw and high-pass-filtered accleration data for all three axes: (a) raw XYZ; (b) high pass XYZ

As presented in Figure 5 the gravity influence is eliminated without loss of informations. Since the phone was almost in an ideal vertical position the gravity impact was largest on the Z axis. The calculation is performed over high-pass-filtered data for the all three axes.

For simulation purposes, smartphone (processor 1.2GHz, Android OS v4.2, accelerometer, GPS) with running application is attached to the windshield using the navigation holder which is presented on Figure 6 a). At this position, suspended mass acceleration is measured. The accelerometer sampling is set to 20ms. Live accelerometer axis signals are plotted on the phone display and stored to files for further analysis. Over vertical (Z) axis calculation (26) is performed in order to calculate interval accumulated vibrations:

$$a_{zRMS} = \sqrt{\frac{1}{n} * (a_{z1}^2 + a_{z1}^2 + \cdots + a_{zn}^2)} \tag{27}$$

where **n** is number of samples, $\mathbf{a_{zi}}$ is Z axis acceleration. During driving locations are saved to KML files, suitable for viewing in GIS software like Google Earth. Marker color represent accumulated vibration level in 10s interval (green < 0.33[m/s^2], 0.33[m/s^2] <= yellow < 0.66 [m/s^2], red >= 066[m/s^2]). Figure 6 b) shows accumulated vibration on Cacak-Uzice relation. Real time calculations were performed beside standard smartphone functions.

a) *b)*

Figure 6 Implemented application usage, a) smartphone position, b) created KML file on Cacak-Uzice relation

6. RESULTS AND CONCLUSIONS

In numerical calculations for the "ramp" and "step" test cases the following values are used:

m_1=28.58 kg, m_2=288.9 kg, λ_1=155900 N/m, λ_2=19960 N/m, β_2=1861.9 Ns/m.

With numerous simulations of systems using different selection of weighting coefficients for the index performance (7) and by result analysis next values are chosen:

$$q_1=1,\ q_2=10,\ q_3=5,\ \rho=2*10^{-10}.$$

By calculating the *Riccatti* equation (9) amplification is calculated:

$$\mathbf{K}= [-70452\ \ 87718\ \ -961\ \ 6917\ \ -158110].$$

Because system values are (14): -2.14, -6.47±j9.79, -57.02±j82.84 according to (24) and the problem of measurements noise with large system bandwidth, we will adopt next reduced observer values: $s_{ir} = -80$, i=1, 2, 3. By solving (23) amplification of the reduced observer is calculated: **L**= [2.52 81.02 -87.42]^T.

At the Figure 5 and Figure 6 responses of the suspension with observer (all states measurable) for excitation "ramp" and the "step" from the road surface, respectively, are shown. It can be seen that the system with the observer has a smaller peak, but in a response to "ramp" negative leap occurs as a result of the new arrangement of zeros and poles of the system. Also, the system response with reduced observer is not significantly better than the response of the system with full observer [4].

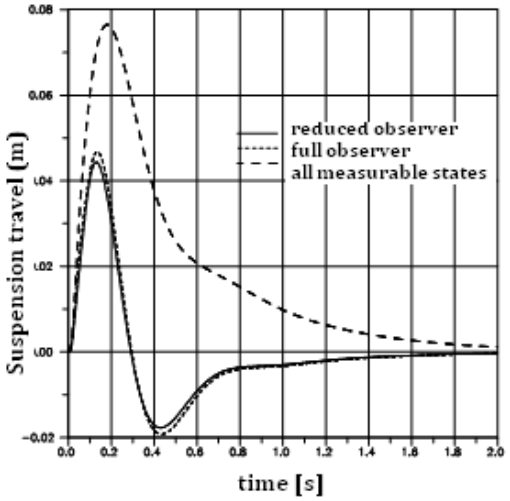

Figure 7 The response of the suspension for the "ramp" from the road surface

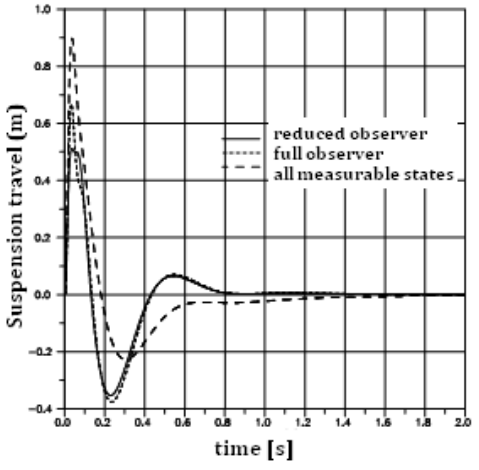

Figure 8 The response of the suspension for the "step" from the road surface

Considering the extremely high sensitivity of the system with reduced observer on noise measurement, we can conclude that the system should be developed with the full observer [4]. Reduced observer in the estimation of the immeasurable states is used less than complete observer because of the output measurement noise (which is random, Gaussian, and which is unavoidable), is not filtered and is even more amplified and directed into the system, as shown in Figure 3. The use of the reduced observer should be avoided because it is better to increase the system with the regulator rather than introducing the system with too big noise.

ACKNOWLEDGMENT

The work presented in this paper was funded by grant no. TR32043 for the period 2011-2016 from the Ministry of Education and Science of the Republic of Serbia.

REFERENCES

[1] ISO 2631-1:1997 - Mechanical vibration and shock -- Evaluation of human exposure to whole-body vibration -- Part 1: General requirements, (n.d.). http://www.iso.org/iso/home/store/catalogue_tc/catalogue_detail.htm?csnumber=7612 (accessed September 8, 2015).

[2] BSI, BS 6841:1987 Guide to measurement and evaluation of human exposure to whole-body mechanical vibration and repeated shock, BSI. (1987). http://www.mendeley.com/catalog/bs-68411987-guide-measurement-evaluation-human-exposure-wholebody-mechanical-vibration-repeated-shoc/ (accessed September 9, 2015).

[3] ASA S2.72-2002/Part 1 / ISO 2631-1:1997 (R2012), (n.d.). http://www.techstreet.com/products/1508686 (accessed September 9, 2015).

[4] Directive 2002/44/EC - vibration - Safety and health at work - EU-OSHA, (n.d.). https://osha.europa.eu/en/legislation/directives/19 (accessed September 9, 2015).

[5] Hand arm vibration - Control of Vibration at Work Regulations 2005, (n.d.). http://www.hse.gov.uk/vibration/hav/regulations.htm (accessed September 9, 2015).

[6] Whole-Body Vibration Building Awareness in SH&E, (n.d.). http://www.asse.org/assets/1/7/030_035_F1Paschold_0411Z.pdf (accessed September 8, 2015).

[7] M.P.H. Smets, T.R. Eger, S.G. Grenier, Whole-body vibration experienced by haulage truck operators in surface mining operations: A comparison of various analysis methods utilized in the prediction of health risks, Appl. Ergon. 41 (2010) 763–770. doi:10.1016/j.apergo.2010.01.002.

[8] K. Plewa, T.R. Eger, M.L. Oliver, J.P. Dickey, Comparison between ISO 2631-1 Comfort Prediction Equations and Self-Reported Comfort Values during Occupational Exposure to Whole-Body Vehicular Vibration, J. Low Freq. Noise, Vib. Act. Control. 31 (2012) 43–53. doi:10.1260/0263-0923.31.1.43.

[9] F. Tüchsen, H. Feveile, K.B. Christensen, N. Krause, The impact of self-reported exposure to whole-body-vibrations on the risk of disability pension among men: a 15 year prospective study., BMC Public Health. 10 (2010) 305. doi:10.1186/1471-2458-10-305.

[10] H. Ayari, M. Thomas, S. Dor, A design of experiments for statistically predicting risk of adverse health effects on drivers exposed to vertical vibrations, Int. J. Occup. Saf. Ergon. 17 (2011) 221–232. doi:10.1016/j.aca.2010.11.024.

[11] B.D.O. Anderson, J.B. Moore, Optimal Control : Linear Quadratic Methods, 1989. http://mirlyn.lib.umich.edu/Record/001956608.

[12] M.M. ELMADANY, Optimal Linear Active Suspensions with Multivariable Integral Control, Veh. Syst. Dyn. 19 (1990) 313–329. doi:10.1080/00423119008968950.

[13] S. Jovanović, M. Ravlić, Design of A Vehicle Active Suspension System, in: 8th Symp. MVM, 1994: pp. 19–24.

[14] A. Mednis, G. Strazdins, R. Zviedris, G. Kanonirs, L. Selavo, Real time pothole detection using Android smartphones with accelerometers, in: 2011 Int. Conf. Distrib. Comput. Sens. Syst. Work. DCOSS'11, 2011. doi:10.1109/DCOSS.2011.5982206.

[15] P. Mohan, V.N. Padmanabhan, R. Ramjee, TrafficSense : Rich Monitoring of Road and Traffic Conditions using Mobile Smartphones, 6th ACM Conf. Embed. Networked Sens. Syst. (2008) 1–29. doi:MSR-TR-2008-59.

[16] J. Eriksson, L. Girod, B. Hull, R. Newton, S. Madden, H. Balakrishnan, The Pothole Patrol: Using a Mobile Sensor Network for Road Surface Monitoring, Proc. 6th Int. Conf. Mob. Syst. Appl. Serv. (2008) 29–39. doi:10.1145/1378600.1378605.

[17] ReactiveX, (n.d.). http://reactivex.io/ (accessed October 5, 2015).